

Architectural Dynamics and Gene Replacement of Coronin Suggest Its Role in Cytokinesis

Yoshio Fukui,^{1*} Sarah Engler,² Shinya Inoué,³ and Eugenio L. de Hostos²

¹*Cell and Molecular Biology, Northwestern University Medical School, Chicago, Illinois*

²*Biochemistry and Cell Biology, Rice University, Houston, Texas*

³*Marine Biological Laboratory, Woods Hole, Massachusetts*

Coronin is a ubiquitous actin-binding protein representing a member of proteins portraying a WD-repeat sequence, including the β -subunits of trimeric G-proteins. Coronin has been suggested to participate in multiple, actin-based physiological activities such as cell movement and cell division. Although the slow growth of coronin deletion mutants has been attributed to a defect in the fluid-phase uptake of nutrients, the exact role of coronin in cytoskeletal organization has not been elucidated. In this study, we examined a role of coronin in cytokinesis by analyzing the effect of coronin deletion on the actin cytoskeleton and its dynamic distribution using a green fluorescent protein (GFP)-coronin fusion protein. We show that GFP-coronin works similarly to natural coronin in vivo and in vitro. In live cells, GFP-coronin was found to accumulate into the cleavage furrow during cytokinesis. The fluorescence pattern suggests its association to the contractile ring throughout cytokinesis. Interestingly, a substantial amount of coronin was also bound to F-actin at the prospective posterior cortex of the daughter cells. We also show that the coronin null cells reveal irregularities in organization of actin and myosin II and divide by a process identical to the traction-mediated cytofission reported in myosin II mutants. Overall, this study suggests that coronin is essential for organizing the normal actin cytoskeleton and plays a significant role in cell division. *Cell Motil. Cytoskeleton* 42:204–217, 1999. © 1999 Wiley-Liss, Inc.

Key words: coronin; cytokinesis; *Dictyostelium*; gene replacement; GFP

INTRODUCTION

Cytoplasmic cleavage has long been studied, but much of its mechanism has not been elucidated. Today, the term “cytokinesis” is used to denote cytoplasmic cleavage by which a cell body cleaves into two [Salmon, 1989]. Normally, cytokinesis accompanies mitotic nuclear division and the cleavage furrow starts to form during anaphase. In this article, we use the term cytokinesis, referring strictly to this mode of cytoplasmic cleavage. Cells occasionally divide into parts in a manner temporally separated from mitosis. This mode of cell division was originally called “cytoplasmic fission” for *Amoeba proteus* [Chalkley, 1935, 1951].

The term “traction-mediated cytofission” was first coined [Fukui et al., 1990] referring to a mode of cytoplasmic cleavage occurring in a *Dictyostelium* mu-

E.L. de Hostos's present address is Tropical Disease Research Unit, University of California, San Francisco, CA 94121.

*Correspondence to: Dr. Yoshio Fukui, Cell and Molecular Biology, Northwestern Medical School, 303 East Chicago Avenue, Chicago, IL 60611–3008. E-mail: y-fukui@nwu.edu

Contract grant sponsor: American Heart Association; Contract grant sponsor: NSF; Contract grant sponsor: NIH; Contract grant number: RO1-GM39548.

Received 10 August 1998; accepted 8 December 1998

tant in which normal myosin heavy chain (mhcA) had been replaced with heavy meromyosin (mhc140) [De Lozanne and Spudich, 1987]. In light of extensive phenotypic similarities, the cytofission in the myosin II mutant of *Dictyostelium* and cytoplasmic fission in *A. proteus* appear to share common mechanisms, i.e., a need of cell-substrate attachment and temporal separation from mitotic nuclear division. Therefore, hereafter, these modes of cell division will be categorically called cytofission. It seems that a recently identified adhesion-dependent cell division by myosin II null cells ("Cytokinesis B") [Zang et al., 1997] represents cytofission because the cells fail completing division in suspension or on a hydrophobic surface.

It has long been known that the initial rounding-up of a cell entering prometaphase is associated with a substantial increase in cortical tension [Mitchison and Swann, 1955; Hiramoto, 1970]. The rounding-up is followed by elongation and constriction, which occur during anaphase and telophase. The "polar relaxation" [Chalkley, 1951] and "astral relaxation" [Wolpert, 1960] theories postulated a decrease in tension at the poles. In contrast, the "equatorial contraction" theory suggests that the major forces are generated by constriction of the furrow due to changes in the cortical gel [Marsland and Landau, 1954], eventually shown to be a circumferential F-actin band ("contractile ring") [Schroeder, 1968]. This latter theory has been experimentally substantiated by Rappaport [1986].

White and Borisy [1983] reevaluated the polar relaxation model and developed a theoretical model that predicted the movement of filamentous components in the plane of the cortex. Actual migration of F-actin in the cortex towards the furrow region has been experimentally demonstrated by Cao and Wang [1990]. Therefore, the polar relaxation and the equatorial contraction mechanisms seem not mutually exclusive. The contractile ring consists of F-actin and myosin II [Fujiwara and Pollard, 1976; Yumura et al., 1984; Mittal et al., 1987; Mabuchi et al., 1988; Schroeder and Otto, 1988; Fishkind and Wang, 1993]. Other components such as α -actinin, fimbrin, and radixin [Fujiwara et al., 1978; Sanger, et al., 1987; Nunnally et al., 1980; Sato et al., 1991, respectively] have also been shown associating with the contractile ring. Recently in *Dictyostelium*, racE, a small GTP-binding protein of the *rho* family, and an IQGAP-related protein, have been indicated to be involved in cytokinesis [Larochelle et al., 1996; Adachi et al., 1997]. These proteins, however, have not been localized to the cleavage furrow. Instead, racE has been reported to be present throughout the cortex in dividing cells [Larochelle et al., 1997].

It is important to note that the mutants defective in seemingly unrelated proteins behave in a manner amaz-

ingly similar to the myosin II deficient cells [Fukui et al., 1990; Zang et al., 1997]; i.e., (1) inability to grow in suspension, and (2) cytofission mode of cytoplasmic cleavage on a substratum [calmodulin, Liu et al., 1992; coronin, de Hostos et al., 1993; cortexillins, Faix et al., 1996; clathrin, Niswonger and O'Halloran, 1997; racE, Larochelle et al., 1996, Gerald et al., 1998; IQGAP-related protein, Adachi et al., 1997]. To date, a significant question remains unsolved: what is the mechanism underlying the cytofission, and does this mechanism play any role in normal cytokinesis?

Coronin is a ubiquitous, 55-kD actin-binding protein originally isolated from *Dictyostelium* [de Hostos et al., 1991] and has been implicated in multiple, actin-based physiological activities, such as locomotion [Gerisch et al., 1995], cell division [de Hostos et al., 1993], phagocytosis [Maniak et al., 1995; Rauchenberger et al., 1997], and macropinocytosis [Hacker et al., 1997]. The precise localization and function of coronin during cytokinesis have not been established.

In the present study, we expressed an S65T-GFP-coronin fusion protein in wild type and coronin null cells, and analyzed its dynamics using a real-time laser confocal microscope. We found that coronin accumulates at the cleavage furrow in two ways: at the contractile ring during early to mid cytokinesis, and at the prospective posterior cortex of the daughter cells during late to end of cytokinesis. The results indicate a role of coronin in cytokinesis, especially at the late phase of division.

MATERIALS AND METHODS

Cells and Cultures

An axenically grown wild type strain Ax2 and its mutants of *Dictyostelium discoideum* were cultured in a modified HL-5 synthetic medium: 5 g Thiotone™ E peptone (Becton Dickinson, Cockeysville, MD), 5 g Bacto™ proteose peptone (no. 2; Difco Laboratories, Detroit, MI), yeast extract (Oxoid, Unipath Ltd., Hampshire, England), 10 g D-glucose, 185 mg Na₂HPO₄, 350 mg KH₂PO₄ in 1 l of distilled water. The S65T-GFP-coronin (GFP-cor) expressing cells were cultured in the medium supplemented with 25 μ g/ml G-418 (Geneticin™; Gibco BRL, Grand Island, NY). For microscopic studies, the cells were propagated in 10-cm plastic Petri dishes. All cultures and observations were made at 22° C.

Generation of Cells Expressing GFP-Coronin

Coronin null cells were generated by gene-disruption as described previously [de Hostos et al., 1993]. The gene-disruption construct used in this study consisted of a coronin cDNA flanking cassette conferring resistance to the antibiotic blasticidin (kindly provided by Dr. H.

Adachi) [Adachi et al., 1994]. The construct was electroporated into wild type Ax2 cells and the transformants were selected in DD-broth20 media [Manstein et al., 1995] containing 5 $\mu\text{g/ml}$ of blasticidin (ICN, Costa Mesa, CA). The coronin null transformants were screened by using a mouse monoclonal anti-*Dictyostelium* coronin antibody as described previously [de Hostos et al., 1993]. Two plasmids expressing modified coronins were constructed: (1) C-terminal of coronin was tagged with a poly (6x)-histidine (His) tail, and (2) the C-terminal was tagged with S65T-GFP (GFP) (Fig. 1A). A full-length coronin cDNA (from start codon to last amino acid codon) was amplified by PCR using primers containing Bam HI restriction sites. The fragment was cloned into the Bam HI site of the expression vector pDXA-3H [Manstein, et al., 1995]. This plasmid carries G418 resistance as a marker and expresses cloned inserts under the control of the constitutive actin-15 promoter. To make a His-tagged construct, the insert was cloned in-frame with a vector segment adjacent to the cloning site, which encodes six C-terminal histidine residues. This construct was further modified by cloning a PCR fragment encoding an S65T variant of the green fluorescent protein [Heim et al., 1995] into an Xho I site blunted with T4 polymerase, which is located between the 3' end of the coronin sequence and the segment encoding the His-tag. The resulting plasmid encodes a coronin whose C-terminal is fused with GFP instead of His.

The two constructs encoding modified coronins and a control pDXA-3H (containing no insert) were transformed into coronin null cells by electroporation [de Hostos et al., 1993]. The transformants were selected in DD-broth20 media containing 20 $\mu\text{g/ml}$ GeneticinTM and 5 $\mu\text{g/ml}$ of blasticidin. Cells from individual transformant colonies were tested for expression of the modified coronins by Western blotting.

Biochemical Characterization of Modified Coronins

GFP-coronin was purified by a method modified from de Hostos et al. [1991]. Briefly, cells were suspended in homogenization buffer containing 1 x complete protease inhibitor cocktail with EDTA (Boehringer-Mannheim Biochemicals, Indianapolis, IN) and lysed in a BioNeb (Glas-Col, Terre Haute, IN) cell homogenizer by two passes at 150 psi of N_2 .

A contracted cell pellet was prepared by adjusting the pH to 7.5 and adding KCl to 20 mM to the 100,000g supernatant fraction of the cell homogenate [de Hostos et al., 1991]. The pellet was extracted sequentially by resuspending with a pipette in homogenization buffer containing 20 mM KCl and increasing concentrations of NaCl (25, 75, 125 mM).

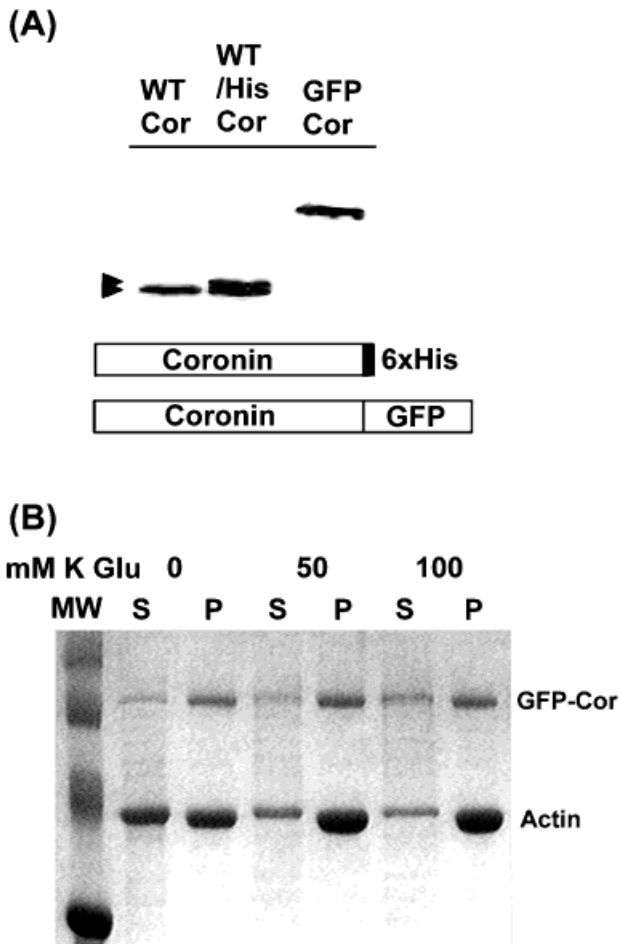


Fig. 1. Expression and purification of GFP-coronin. **A:** Western blot probed with an anti-coronin monoclonal antibody of proteins from wild-type Ax2 cells (WT-Cor), wild-type cells expressing endogenous (natural) coronin, and a histidine-tagged coronin (arrowheads; WT/His-Cor), and coronin null cells expressing GFP-coronin (GFP-cor). For details about the construct, see Materials and Methods. **B:** Co-sedimentation of GFP-coronin with F-actin. GFP coronin was incubated with actin under polymerizing conditions with different concentrations of potassium glutamate (K-Glu). After polymerization, the samples were centrifuged and supernatant (S) and pellet (P) fractions were collected and analyzed with SDS-PAGE.

GFP-coronin was identified in the different fractions by Western blotting using anti-coronin antibodies. Fractions containing a high concentration of GFP-coronin were collected and dialyzed against G-actin buffer (2 mM Tris-HCl, 0.2 mM CaCl_2 , 0.2 mM ATP, 0.01% NaN_3 , pH 8.0). Final condensation and purification were done with a filter concentrator with a 50 kD molecular weight cut-off (Microcon 50; Amicon, Beverly, MA). GFP-coronin was used in F-actin co-sedimentation assays as described previously [de Hostos et al., 1991]. GFP-coronin (2.5 μM) was incubated with actin (5 μM) in polymerization buffer (10 mM imidazole-HCl, 2 mM MgCl_2 , 1 mM EGTA, pH. 7.6). Under this condition,

actin shows measurable polymerization in the absence of KCl [Scheel et al., 1989]. After a 30-min incubation at room temperature, coronin and actin mixture was sedimented in cold for 30 min in an airfuge (Beckman Instruments). The reaction mixture was supplemented with an increasing concentration of K-glutamate (0, 50, 100 mM) to test the effect of ionic strength on the interaction between GFP-coronin and F-actin. K-glutamate was used because it has been reported to be less chaotropic and more natural in cytoplasm than NaCl [Richey et al., 1987].

Characterization of Physiological Activity of GFP-Coronin in Live Cells

To measure the growth rate in suspension culture, cells were grown in 50-ml flasks containing DD-broth20 media on an orbital shaker at room temperature. The growth rate was determined by counting cells at various time points using a hemocytometer. To determine the number of nuclei per cell, cells were allowed to attach to ethanol-sterilized cover slips and then grown in submerged culture for two days. The cells were fixed for 10 min with -20°C methanol containing 1% formalin. The cells were stained with 0.1 $\mu\text{g/ml}$ of 4',6'-diamidino 2-phenylindole (DAPI) (no. D-1388; Sigma) in Tris-buffered-saline containing 0.1% Tween-20. The image was recorded using a fluorescence microscope (Axiophot; Carl Zeiss, Thornwood, NY) equipped with a video camera (CCD100; DAGE-MTI, Michigan City, IN).

Immunofluorescence Microscopy

Samples were observed under a fluorescence microscope (Axioskop-50; Carl Zeiss) equipped with a 63x/NA 1.4 plan apo oil immersion objective lens. The image was recorded through a full frame digital cooled CCD camera (PXL; Photometrics, Tucson, AZ), installed with a 12-bit, full frame image sensor (KAF 1400 chip; Eastman Kodak, Rochester, NY). Using an objective micrometer (no. 473390; Carl Zeiss), we established that the X and Y dimensions for each pixel on the chip were 106 and 101 nm, respectively [Yumura and Fukui, 1998]. The actual spatial resolution was limited by the microscope system whose theoretical spatial resolution is about 250 nm for the epifluorescence system (i.e., 227 nm for FITC, and 266 nm for TRITC).

For immunofluorescence staining, cells were fixed with methanol containing 1% formalin for 5 min at -15°C , then washed with phosphate-buffered saline (PBS: 138 mM NaCl, 2.5 mM KCl, 8 mM Na_2HPO_4 , 1.5 mM KH_2PO_4 , pH 7.2) for 10 min. The culture medium of the hybridoma secreting anti-*Dictyostelium* coronin (no. 2-B5-10) [de Hostos et al., 1991], or anti-*Dictyostelium* myosin II (DM2) [Yumura et al., 1984] was used as the primary antibody. The samples were incubated for 30 min

at 36°C . The samples were then washed with PBS for 10 min. Secondary antibody was applied to the samples and incubated for 30 min at 36°C . The stained samples were then washed with PBS for 10 min, followed by a brief rinse with distilled water to remove salts. For the double staining with tetramethylrhodamine isothiocyanate-phalloidin (rh-ph), rh-ph (no. R-415; Molecular Probes, Inc., Eugene, OR) was mixed with the secondary antibody at a final concentration of 3 μM . The samples were mounted with the mounting medium made of a 1:2:4 mixture of polyvinyl alcohol, glycerol and PBS containing 1% (w/v) of an anti-oxidant DABCO (diazabicyclo [2.2.2.] octane) (Aldrich Chemical Co., Milwaukee, WI).

Real-Time Confocal Analysis

Video rate confocal images were generated by a real-time spinning-disk confocal unit (CSU-10; Yokogawa Electronic Corp., Tokyo, Japan) equipped with an argon ion laser (Omnichrome, Chino, CA) as described [Inoué and Inoué, 1996]. The unit was installed on a Nikon inverted microscope (E800; Nikon Inc., Melville, NY) also equipped with a standard epifluorescence and phase-contrast units. We used a 60x/1.4 N. A. or 100x/1.4 N. A., plan apo oil immersion objective lens (Nikon Inc.). The image was integrated on-chip for 6 to 15 video frames (0.2–0.5 second) in a chilled CCD camera (C-5985; Hamamatsu Photonics, K.K., Hamamatsu City, Japan). Image acquisition was controlled by an integrated image acquisition and analysis system (MetaMorph; Universal Imaging Corporation, West Chester, PA), using an electric shutter driver (UniBlitz SD-10; Vincent Associates, Rochester, NY). The image was analyzed using the MetaMorph program. To quantify the gray level depth, the intensity was scanned along a line of 10-pixel width.

For observation, an aliquot of suspension of growth phase cells was placed on a 22 x 22-mm² glass coverslip (no. 1, 170- μm -thick; Corning Glass Works, Corning, NY), and allowed to settle for 1 h. All the observations were made using the observation chamber described below.

Observation Chamber

Thin agarose coverslips were made by the method described previously [Fukui and Inoué, 1991]. Briefly, an 8 x 8 mm² agarose sheet saturated with Bonner's salt solution (10 mM NaCl, 10 mM KCl, 3 mM CaCl_2) was draped over the cells. The coverslip was then turned over and placed on a slide glass supported by a 170- μm -thick spacer made of filter paper (no. 541; Whatman, Hillsboro, OR), and sealed with VALAB (a 1:1:1 mixture of Vaseline, lanolin and bee's wax) [Fukui and Inoué, 1997]. The samples were incubated at 22°C for 2–3 h until many mitotic figures were observed.

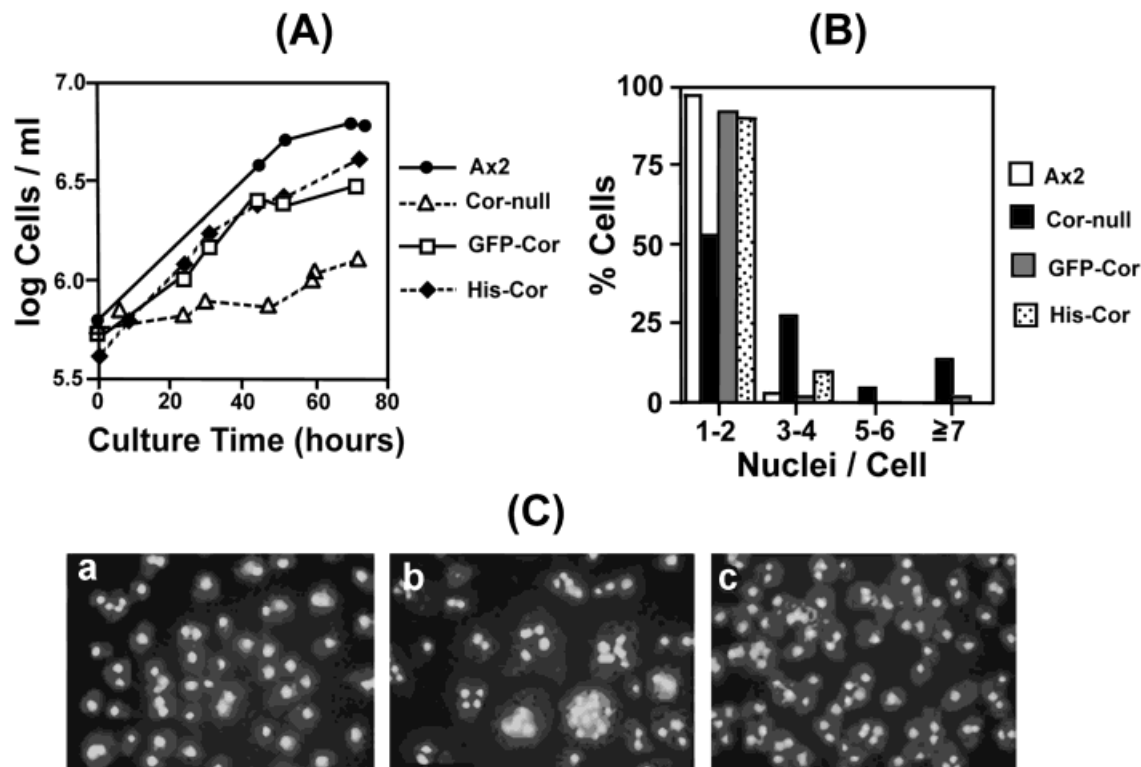


Fig. 2. Phenotypic rescue of coronin null cells by modified coronins. **A:** Growth rate of parent strain (Ax2), coronin null mutants (Cor-null), and null cells expressing histidine (His-) or GFP-tagged coronin (GFP-Cor) cultured in suspension. The division of coronin null cells is severely impaired but this defect is complemented by expressed His- or GFP-coronin. **B:** The frequency of multinucleated cells in cultures of

Ax2, coronin null, and null-cells expressing His- or GFP-coronin. Most Ax2 cells are uninuclear, while many null-cells contain several nuclei. This defect is rescued by expressed His- or GFP-coronin. **C:** Micrographs showing the nuclear profile of Ax2 (a), coronin null (b), and null-cells expressing GFP-coronin (c). The cells were stained with DAPI.

RESULTS

Phenotypic Rescue of Coronin Null Cells With Modified Coronins

In order to verify that GFP-coronin is physiologically active, we first examined its actin-binding activity *in vitro*. GFP-coronin was purified (Fig. 1A) and used in actin co-sedimentation assay similar to those done previously for native coronin [de Hostos et al., 1991]. Neither coronin nor GFP-coronin alone sedimented during the centrifugation when actin was absent (data not shown). When incubated with actin, GFP-coronin co-sedimented with F-actin even when ionic strength was increased by supplementing with 100 mM K-glutamate (Fig. 1B), as has been shown previously for native coronin [de Hostos et al., 1991]. Overall, GFP-coronin showed identical property to natural coronin of interaction with F-actin under our experimental conditions.

Next, to test the activity of the fusion protein *in vivo*, coronin null cells were transformed with a control plasmid or a plasmid encoding a coronin modified with either a C-terminal histidine tail (His-cor), or a fusion with GFP (GFP-cor). The coronin null cells can divide on

solid substrata by cytofission in 5–15 min (data not shown). This speed is similar to that of myosin II null (*mhcA*) cells. The ability of the modified coronins to complement the lack of natural coronin was evaluated by: (1) examining the growth rate of cells in suspension, and (2) by counting the number of nuclei per cell for cells grown on a glass surface (Fig. 2). The results demonstrate that cells expressing His-cor or GFP-cor grow much faster and more normally than the cells transformed with the control plasmid (Fig. 2A) at a rate comparable to that of the wild-type Ax2 cells.

The above results are reflected by the distribution of the number of nuclei in these cells (Fig. 2B). Cells expressing the modified coronins have fewer multinucleated cells than the cells transformed with the control plasmid, with a numerical distribution similar to that of the wild-type Ax2 cells. The nuclear staining of the wild type (Fig. 2C-a), coronin null cells with (Fig. 2C-b) or without expressed GFP-coronin (Fig. 2C-c) further demonstrates the complementation of coronin deletion by GFP-coronin. These results demonstrate that the modified coronins complement the lack of natural coronin, and that

the modified coronins behave biochemically in a manner similar to the natural protein. Thus, GFP-coronin fusion protein should provide a physiologically accurate picture of the subcellular distribution of natural coronin.

In Situ Dynamics of GFP-Coronin

Since coronin has been localized to macropinosomes and implicated in the fluid phase uptake of medium, we first examined the dynamics of GFP-coronin in this process. The evidence shows, as reported by Hacker et al. [1997], that GFP-coronin indeed localizes to the cortical area exhibiting morphological changes typical of fluid phase pinocytosis (Fig. 3). The initial cortical structure represents a "crown" [de Hostos et al., 1991], confirming a recently proposed model that the formation of macropinosomes is brought about by morphological change of the crown [Hacker et al., 1997]. The three representative sequences show that a crown transforms into a cup (large arrows; Fig. 3-1a, 2a, 3a) and the cup closes within 30 seconds (Fig. 3-1d, 2c, 3b). The diameter of vesicles surrounded by GFP-coronin (approximately 1.5 μm ; arrowheads in Fig. 3-2f) is similar to the average diameter of the reported macropinosomes (1.6 μm) [Hacker et al., 1997]. These results indicate that GFP-coronin is capable of dynamically integrating into the cortical cytoskeleton and its incorporation does not cause adverse effects on the F-actin activity in vivo.

Coronin Distribution on the Cytoskeleton of Dividing Cells

The original immunofluorescence study by de Hostos et al. [1993] localized coronin, in thick cells fixed with picric acid/formaldehyde, to the polar lamellipodia of dividing cells, but not to the cleavage furrow. In the present study, we analyzed the intensity profile of the images acquired at high spatial and gray level resolutions. The cells were prepared by the agar-overlay method so that they were nearly two-dimensional, with an average thickness of about 3 μm [Fukui and Inoué, 1991, 1997]. Under these conditions, the fluorescence intensity is closely related to the relative concentration of GFP-coronin. Under these conditions coronin shows the highest intensity at the polar lamellipodia, but also a notable accumulation at the furrow region (Fig. 4A-a'-c': white brackets). The evidence for the rich accumulation of coronin in the leading edge confirms previous observations [de Hostos et al., 1991; Gerisch et al., 1995; Maniak et al., 1995; Hacker et al., 1997].

The intensity profiles of coronin in the cells at early- (Fig. 4B-a''), mid- (Fig. 4B-b''), and late- (Fig. 4B-c'', d'') cytokinesis demonstrate that the amount of cytoskeleton-bound (remained after fixation and extraction) coronin is in fact higher in the furrow region than in the ground

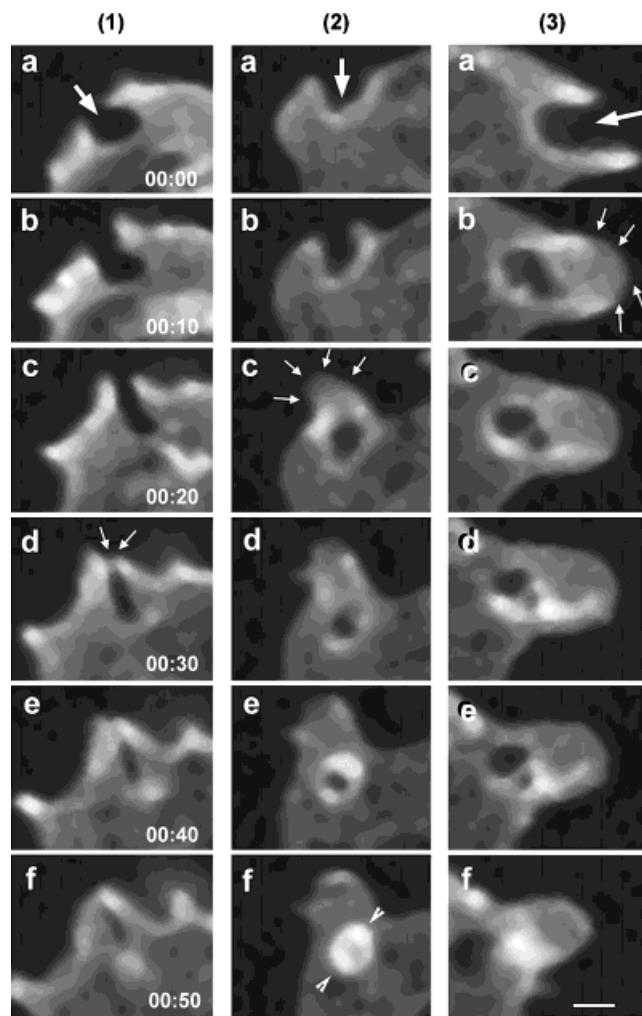


Fig. 3. Representative sequences showing the dynamic redistribution of GFP-coronin in the cell cortex exhibiting macropinocytotic activity. Initially, GFP-coronin accumulates in the cortex surrounding the cup (large arrows: 1-a, 2-a, 3-a). The opening was sealed with the plasma membrane (small arrows: 1-d, 2-c, 3-b), and the vacuole was internalized (2-d, 3-c). GFP-coronin occasionally showed an intense circular fluorescence whose diameter was about 1.5 μm (arrowheads: 2-f). This datum demonstrates that GFP-coronin dynamically integrates into the cortical F-actin and its incorporation does not inhibit the normal F-actin activity. Time, min:sec. Scale bar = 1 μm .

cytoplasm. The approximate increase in the concentration of coronin at the furrow in these images was 61% (Fig. 4B-a''), 69% (Fig. 4B-b''), and 45% (Fig. 4B-c''), relative to the ground cytoplasm (indicated by the double-headed arrows in Fig. 4B-a''-d''). Our statistical analysis shows that the average increase is $60 \pm 3.5\%$ ($n = 17$), $73 \pm 3.7\%$ ($n = 16$), and $37 \pm 7.3\%$ ($n = 23$), respectively, for early-, mid-, and late-cytokinesis. Interestingly, the distribution of coronin suggests the orientation of a fibrous structure in the furrow region perpendicular to the pole-to-pole axis, indicating its association with the contractile

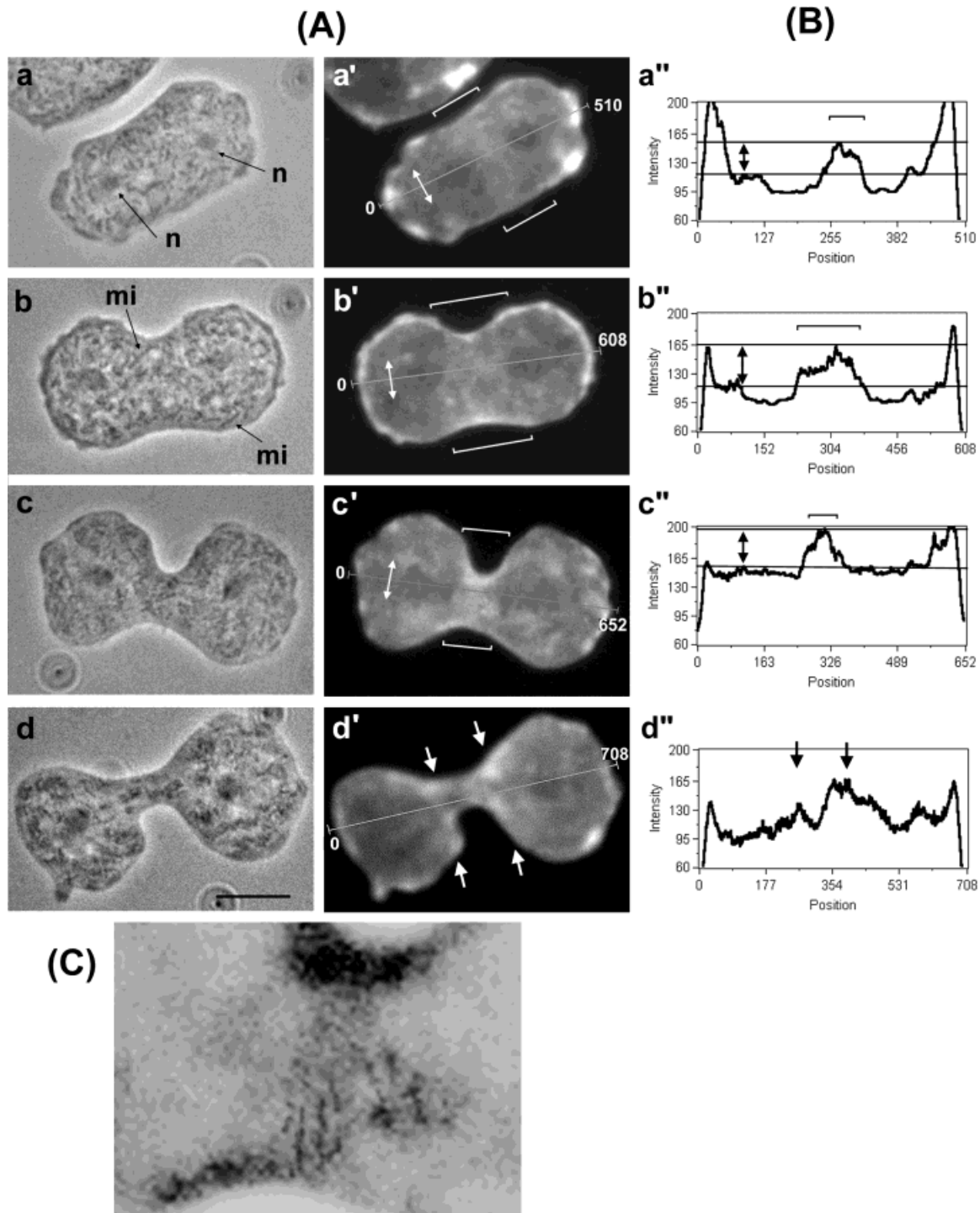


Fig. 4. Phase-contrast and immunofluorescence micrographs (A), intensity profile (B), and the enhanced image (C) showing the coronin distribution in dividing cells. The cells were in early- (a), mid- (b), and late- (c,d) cytokinesis. The cells were fixed and stained with monoclonal anti-*Dictyostelium* coronin, followed by FITC-goat anti-mouse IgG. Intensity was measured for a 10-pixel-wide scan lines marked in a'–d', and their profiles are shown in corresponding panels, a''–d''. Position is indicated by pixel numbers along the lines. The profiles demonstrate that coronin shows a conspicuous localization in the cleavage furrow (brackets). The intensity is higher than the base level

in the ground cytoplasm (double-headed arrows) by 61% (a''), 69% (b''), and 45% (c''). Note that the pattern of coronin staining at the furrow seems fibrous and oriented perpendicular to the axis of cell division (c'). The fibrous structures are clearly shown in C after image processing (i.e., the gray value was non-linearly enhanced, speckles were removed, and the contrast was inverted). Note that the posterior cortex of presumptive daughter cells shows a significantly higher fluorescence (arrows in d''). Bracket: cleavage furrow, n: nucleus, mi; mitochondrion. Scale bar = 5 μ m.

ring (Fig. 4A-b', c'). The fibrous organization is more clearly shown after vigorous image processing (Fig. 4C). In late-cytokinesis, the distribution profile of coronin becomes unorganized as the furrow is stretched and disoriented (Fig. 4A-d-d''). It is noteworthy that, at this phase, coronin remains associated with the cortex of prospective daughter cells (Fig. 4A-d': arrows). The intensity profile of this cell demonstrates that the amount of cortical coronin at the furrow is even higher than at the polar lamellipodia (Fig. 4A-d'': arrows).

GFP-Coronin Distribution in the Cleavage Furrow of Live Amoebae

The cells expressing GFP-coronin performed apparently normal cytokinesis. We have observed a total of 25 cells performing cytokinesis, and successfully recorded 18 dynamic sequences. During the initial observation, we noticed that when the excitation light was too strong, the cells rounded up and stopped cytokinesis. Therefore, we adjusted the excitation intensity by attenuating the laser power and/or inserting a neutral density filter. The expression level of GFP-coronin was also a major factor affecting the photosensitivity. In all successful sequences, the GFP-coronin expressing cells completed cytokinesis within 20 min. This speed is comparable with the previously reported speed of cytokinesis of wild type cells as determined by high-resolution DIC observation [Fukui and Inoué, 1991]. In the following, the raw data were acquired as 8-bit images so that the actual dynamics can be ascertained with considerably higher clarity in their playback than can be seen in selected still displays. (Movie can be seen on WEB site: <http://pubweb.nwu.edu/~yoshifk/fukui.html>.)

In a representative cell, GFP-coronin most dramatically accumulated into polar lamellipodia (arrowheads: Fig. 5a). This localization agrees with the original immunofluorescence localization of coronin [de Hostos et al., 1993]. Immunofluorescence microscopy shows an intense accumulation of coronin in the eupodia, recently discovered actin-rich cortical structures that are thought to be responsible for cell-substrate anchorage [Fukui and Inoué, 1997; Fukui et al., 1997]. GFP-coronin also becomes integrated dynamically into this structure (arrowheads: Fig. 5q, t). GFP-coronin was also distributed diffusely throughout the cytoplasm. Although a part of this diffuse fluorescence is thought to represent unbound molecules, its real origin has not been determined. The cytoplasm exhibits dark spots that indicate the presence of organelles from which GFP-coronin is excluded.

In addition to the above localization, GFP-coronin shows a notable accumulation into the cleavage furrow (arrows: Fig. 5c–e). The level of accumulation in the furrow was 25–30% higher than the general ground cytoplasm (data not shown; see Fig. 6 for more detailed

analysis). Interestingly, the accumulation of GFP-coronin in the furrow remained high until late cytokinesis (Fig. 5r,s) and in the posterior cortex of presumptive daughter cells (arrows: Fig. 5r–t). This observation is unique and noteworthy, because to date coronin has not been located to the posterior region of migrating or dividing cells [de Hostos et al., 1991, 1993; Gerisch et al., 1995]. This localization of coronin was consistent in all the sequences recorded.

The relative intensity of GFP-coronin was measured at higher magnification (Fig. 6). At this magnification, the image allows us to identify some organelles such as nucleus (n), mitochondria (mi), and contractile vacuoles (cv) (Fig. 6A). To simplify the analysis, the intensity was first scanned along a 10-pixel-wide line along the cleavage furrow (Fig. 6B). This method eliminates complicated dynamic signals derived from other sources including coronin-rich polar lamellipodia and eupodia (thin arrows: Fig. 6A-d–f; arrowheads: d, i). The data show that GFP-coronin exhibits a high accumulation in the *lateral* cortex of the furrow region, indicating its circular organization surrounding the entire cortex (large arrows: Fig. 6A-e; thin arrows: Fig. 6B). Next, the intensity was scanned along the pole-pole axis in selected images (Fig. 6C). This measurement showed that the relative increase in the intensity in the cleavage furrow, relative to the ground cytoplasm (double-headed arrows: Fig. 6A-e, j), was 16% (Fig. 6C-e'') and 27% (Fig. 6C-j''), respectively, in this representative cell.

Although conspicuous, these measurements only revealed a relatively small increase in concentration of coronin in the furrow, as compared to immunofluorescence samples (Fig. 4A). The reason for this difference can be explained by the fact that the immunofluorescence sample was fixed and extracted, thus eliminating the free coronin background; while the GFP-coronin image reflects its distribution of coronin in the whole live cytoplasm. Therefore, a high fluorescence of the free GFP-coronin masks some of the signal from cytoskeleton-bound coronin.

The conclusion from this analysis at high magnification is that GFP-coronin exhibits a considerable accumulation in the cleavage furrow. GFP-coronin continues to localize in the furrow throughout cytokinesis (arrows: Fig. 6B–j). We consistently observed a high signal also at the presumptive posterior cortex of daughter cells in all sequences.

Cytoskeletal Organization of Coronin Null Cells

To decipher the effect of the absence of coronin on the cytoskeleton, we examined the organization of F-actin

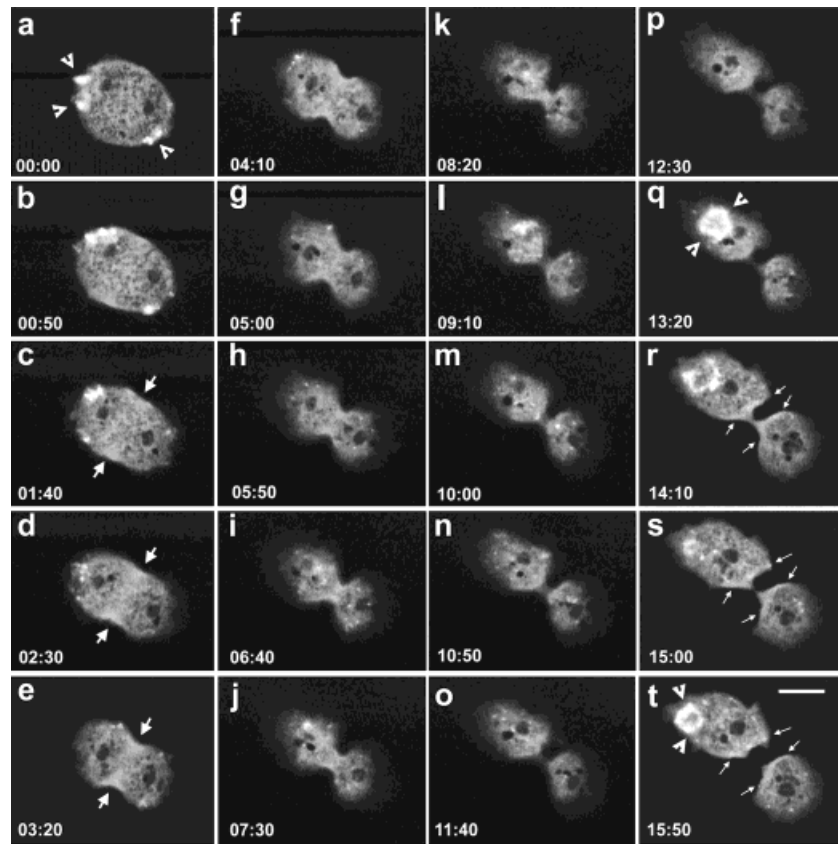


Fig. 5. Digital image panels illustrating the dynamics of GFP-coronin in a dividing cell. The original images were acquired every 10 seconds, and this figure shows only one image out of five. GFP-coronin shows the highest, intense fluorescence at the polar lamellipodia (arrowheads; a). The appearance of the cytoplasm is spotty due to the presence of organelles. GFP-coronin also accumulates into eupodia (arrowheads; q, t). There is a notable accumulation of GFP-coronin in the furrow

region during the mid (large arrows: c–e) and late phase (small arrows; r, s). This distribution is maintained after a complete separation of the daughter cells (t). Note that, in the area of high intensity (e.g., eupodia: arrowheads in q), the fine detail cannot be resolved due to gray level saturation. The complete sequence can be seen in <http://pubweb.nwu.edu/~yoshifk/fukui.html>. Time, min:sec. Scale bar = 5 μ m.

and myosin II by immunofluorescence in null cells manifesting abnormal cytoplasmic cleavage (i.e., those exhibiting “cytofission”). In wild type cells, F-actin is localized in pseudopodia, eupodia, and the cortex primarily surrounding the posterior cortex, while myosin II is excluded from the anterior cell body (Fig. 7a', a''). We find that the organization of the actin cytoskeleton is partially altered in the null mutant (Fig. 7b–e). In an interphase cell (Fig. 7b–b''), the rh-phalloidin staining shows a high intensity in leading edges and pseudopodia (arrowheads: b') as is seen in wild-type cells. However, the position of eupodia is unusual; the cell produces these structures in the center of the cell (small arrows: Fig. 7b'). This is in marked contrast to the position of eupodia in wild type cells, in which eupodia are always formed at the base of developing pseudopodia (arrows: Fig. 7a'). The organization of myosin II in this cell appears normal with respect to its exclusion from the pseudopodia (Fig. 7b'').

In cells dividing by cytofission (Fig. 7c–e), the organization of F-actin (Fig. 7d', e') is strikingly similar to that observed in the myosin II mutant (*mhcA-*) expressing truncated myosin II heavy chain [Fukui et al., 1990]. While leading edges and lamellipodia always show notable accumulation of F-actin, the appearance of F-actin in the cytoplasm is variable. This variation seems to reflect the organizational variance of F-actin in different cells; i.e., F-actin structure is thought to be conspicuous only when it is organized into thick bundles. In fact, in some case, myosin II in the coronin null cells co-localizes with these F-actin structures (arrowheads: Fig. 7d'), manifesting an unmistakably prominent fibrous organization (Fig. 7d''). Overall, the evidence of this study demonstrated that deletion of coronin causes a significant alteration in actin organization, indicating a vital role of coronin in organizing F-actin during cell locomotion and cytokinesis.

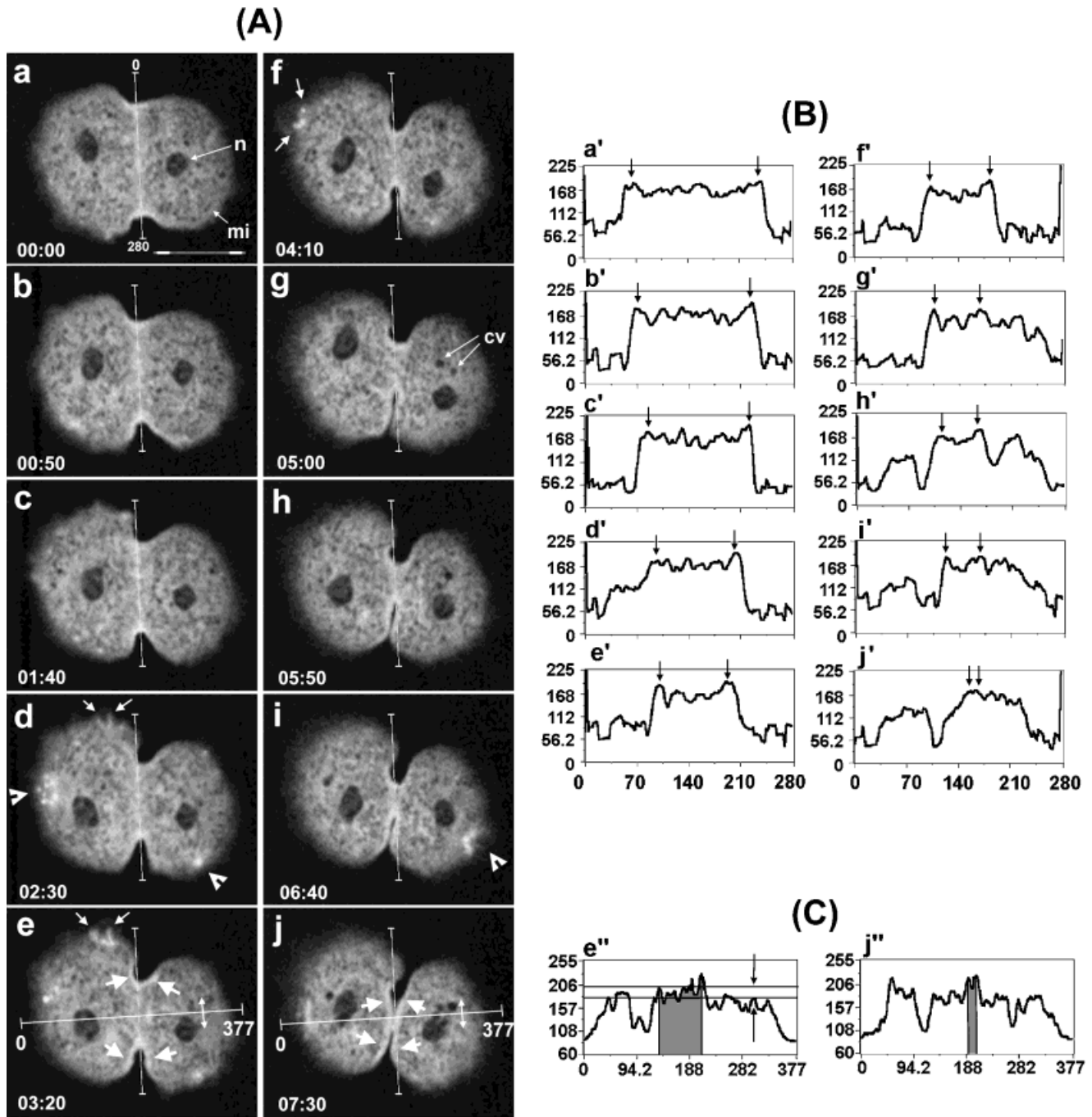


Fig. 6. The distribution and intensity profile of GFP-coronin during cytokinesis. **A:** Fluorescence image sequence. As in Figure 5, the actual images were acquired every 10 seconds. GFP-coronin exhibits a spotted pattern in the cytoplasm, due to its exclusion from organelles, including nucleus (n), mitochondria (mi), and contractile vacuoles (cv). The highest intensity was in the eupodia (arrowheads; **d**, **i**), and the crown-like cortical structures (two small arrows; **d**–**f**). Note that the cortex in the furrow region shows a notably higher fluorescence (large arrows; **e**), and this distribution is maintained after completion of

cytokinesis (arrows; **j**). **B:** The intensity profile in the cleavage furrow along a line perpendicular to the pole-pole axis, showing a significant accumulation of coronin in the furrow. The side view of the cortex (arrows) shows the highest intensity due to thick path length. **C:** The intensity profile along the division axis. An increase in the intensity relative to the ground cytoplasm is 16% (**e''**) and 27% (**j''**). Movie: <http://pubweb.nwu.edu/~yoshifk/fukui.html>. Time, min:sec. Scale bar = 10 μ m.

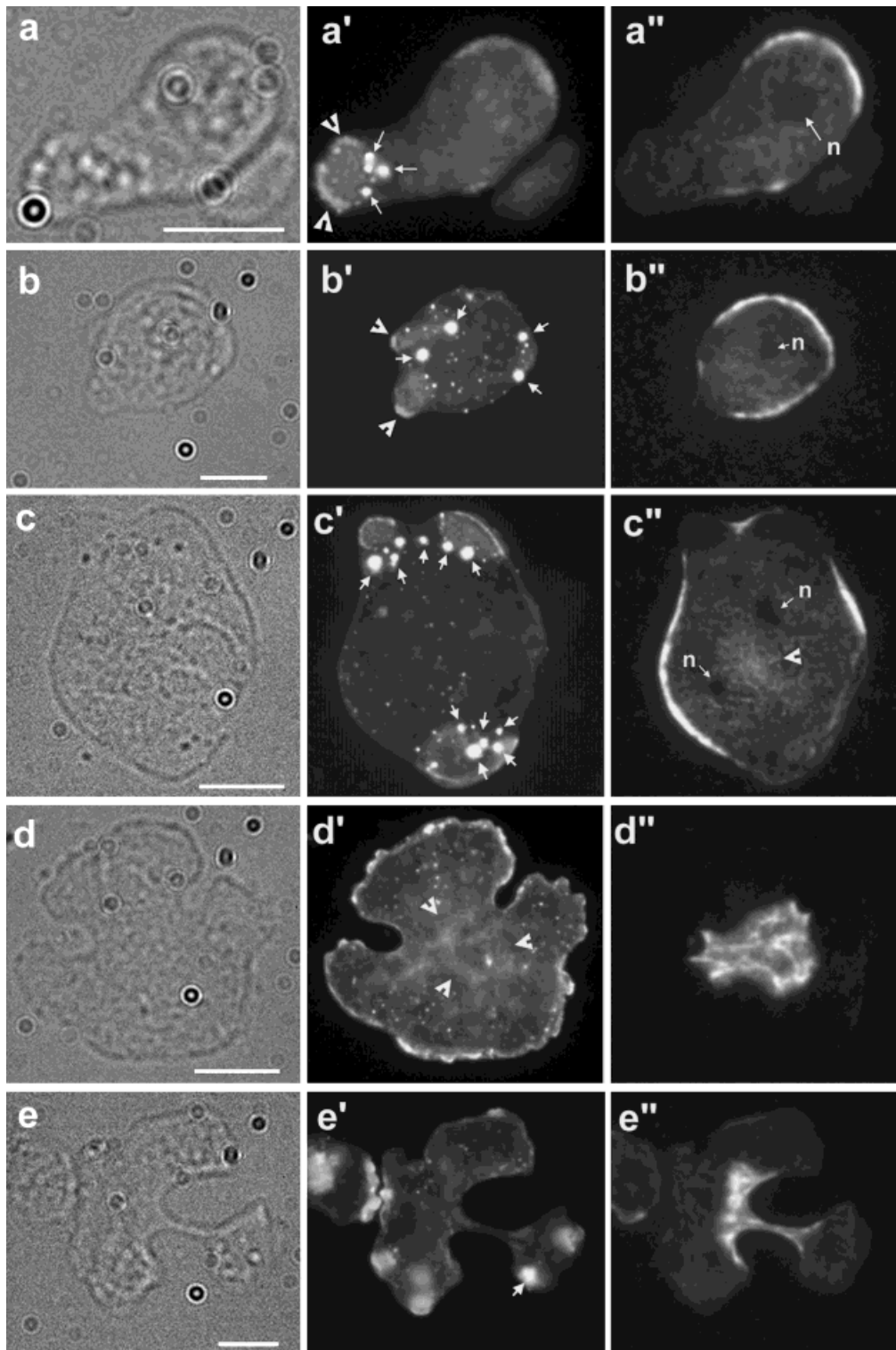


Fig. 7. The immunofluorescence localization of F-actin and myosin II in wild type and coronin null cells. The panels represent interphase cells (a,b) and cells in different stages of cytofission (c–e). The samples were double-stained with rh-phalloidin (a'–e') and a mouse monoclonal anti-*Dictyostelium* myosin II (a''–e''). In wild type (a–a''), actin primarily assembles into F-actin in pseudopodia (arrowheads), posterior cortex, and eupodia locating at the base of pseudopodia (arrows). Interphase coronin null cells have unusual F-actin organization as

represented by centrally located eupodia (b': arrows). In dividing cells, F-actin forms a fibrous network in the center of a multipolar cell (arrowheads: d'). Myosin II is clearly associated with the F-actin network during the middle stages of cytofission (d''). F-actin exhibits an extensive accumulation in eupodia (arrows: c', e'). Note that the myosin II staining is completely negative in the eupodia. Scale bar = 5 μ m.

DISCUSSION

GFP-Coronin Serves as a Reliable Probe to Examine Live Dynamics of F-Actin

Coronin is one of the actin-binding proteins that bind F-actin in a Ca^{2+} - and pH-independent manner [de Hostos et al., 1991]. In the present study, we showed that both His-cor and GFP-coronin maintain the actin-binding activity similar to that of wild type coronin. We also showed that, when expressed in live amoebae, GFP-coronin is distributed in crown, pseudopodia, and macropinocytotic cups, similar to the localization of natural coronin shown in previous studies [de Hostos et al., 1991; Gerisch et al., 1995; Maniac et al., 1995; Rauchenberger et al., 1997]. We further confirmed that the modified coronins are active in live cells by their ability to rescue coronin null cells. From these data, we believe that GFP-coronin provides a reliable marker for investigating the in vivo distribution of coronin.

Does *Dictyostelium* Form a Contractile Ring?

A large body of evidence has been accumulated that demonstrates the presence of a circumferential, contractile ring at the cleavage furrow in a wide variety of cell types. In addition to electron microscopy, immunofluorescence evidence has been provided in fibroblasts [Fujiwara and Pollard, 1976], sea urchin and newt eggs [Schroeder and Otto, 1988; Mabuchi et al., 1988], *Dictyostelium* [Kitanishi-Yumura and Fukui, 1989; Gerald et al., 1998], and rat kidney cells [Fishkind and Wang, 1993]. Some questions that have not been fully clarified, however, are the nature of the additional molecular components and the architectural organization of the contractile ring, as well as the mechanism by which this structure is regulated to form and perform its activities. In *Dictyostelium*, only one actin-binding protein, myosin II, has previously been localized to the cleavage furrow, while other components such as myosin I [Fukui et al., 1989], α -actinin [Fukui, 1993], cortexillins [Faix et al., 1996], fimbrin [Prassler et al., 1997], and cofilin [Aizawa et al., 1997] have been shown not to localize in this region. In the present study, we demonstrated that coronin, indeed, accumulates at the cleavage furrow, probably by associating with the contractile ring.

In live cells, neither GFP-actin [Neujahr et al., 1997] nor micro-injected rhodamine-actin [Yumura and Fukui, 1998] exhibits a prominently fluorescent contractile ring. The primary reason for this is thought to be that the background fluorescence from soluble G-actin swamps-out the signal from the F-actin in the contractile ring. The evidence that micro-injected FITC-phalloidin exhibits a more prominent distribution at the furrow in live cells [Fukui et al., 1999] supports this possibility since this probe only binds F-actin and not to G-actin.

In vitro, in *Dictyostelium*, coronin has been shown to bind F-actin, in a Ca^{2+} and pH-independent manner [de Hostos et al., 1991]. Coronin-like proteins from other organisms have also been shown to bind F-actin [reviewed in de Hostos, 1998]. Thus, coronin can be considered as a useful probe for identifying the presence of F-actin in vivo as well. Our detection of coronin at the cleavage furrow in live amoebae, indeed, supports our conclusion that F-actin is organized in the cleavage furrow building the contractile ring.

How Does Coronin Integrate Into Actin Cytoskeleton During Cytokinesis?

Our immunofluorescence staining and the cross-sectional view of GFP-coronin distribution in live cells demonstrate that coronin exhibits a notable accumulation into the cleavage furrow (Figs. 4, 6). The immunofluorescence image implies the occurrence of a fibrous, circumferential architecture, aligned perpendicular to the division axis (Fig. 4C), which fits our concept of the contractile ring [Schroeder, 1968; Rappaport, 1986; Fukui, 1993; Fishkind and Wang, 1993]. It seems very likely that this structure represents the organization of coronin associated with the F-actin of the contractile ring. In live cells expressing GFP-coronin (Fig. 5), we could not see the circumferential “band” in plain view. As discussed earlier, this is probably due to the swamping of the weak signal by the background fluorescence of GFP-coronin that is present throughout the cytoplasm.

We observed that the fluorescence of cortical GFP-coronin remains high even after a complete cytoplasmic division (thin arrows: Fig. 5-r–t; thick arrows: Fig. 6A–j). This coronin-containing structure in the posterior cortex appears to be a product of a remnant of the contractile ring. To date in migrating cells, coronin has been primarily localized to anterior pseudopodia, crown, macropinocytotic cups, and eupodia, but not to the posterior cortex. This distribution is consistent in all published images of the localization of coronin [de Hostos et al., 1991; Gerisch et al., 1995; Maniac et al., 1995; Hacker et al., 1997; Fukui et al., 1997]. In other words, the observed high accumulation of coronin to the posterior cortex is unique to dividing cells. We suggest that this subset of coronin may play a crucial role in completion of cytokinesis, since the coronin deletion mutant divides inefficiently, resulting in production of multinucleated cells [de Hostos et al., 1993].

What Is the Role of Coronin In Cytokinesis?

In this study, we demonstrated that the coronin deletion mutants divide primarily by cytofission, a mode typical of myosin II mutants [Fukui et al., 1990]. In the coronin null cells, we found that the actin-cytoskeleton exhibits an irregular organization to which myosin II

co-localizes (Fig. 7-d', d''). We also demonstrated strong similarities between coronin and myosin II deletion mutants in the mode of division. Among many actin-binding proteins in *Dictyostelium*, myosin II and coronin are the only two proteins localized so far to the cleavage furrow, indicating a possibility that these proteins are involved in the same, or serial, processes that lead to normal cytokinesis. While the assembly and localization of myosin II have been shown to be regulated by dephosphorylation of the heavy chain [Egelhoff et al., 1993], other cellular factors could also be involved.

To date, little is known about the biochemical properties of coronin [de Hostos et al., 1991]. However, structural, genetic, and biochemical evidence have shown that WD-repeats are involved in mediating protein-protein interactions [reviewed in de Hostos, 1998]. If coronin is binding to F-actin and simultaneously to other proteins, this could result in cross-talk between different actin-binding proteins. It is tempting to speculate that such a mechanism could be involved in the localization of coronin to the cleavage furrow, and to the disruption of the actin cytoskeleton in coronin null cells performing cytofission.

The results of this work suggest a possible interplay between coronin and myosin II that deserves further investigation. We speculate that, while myosin II works as a mechanochemical transducer generating contractile forces, coronin may play a role in preserving the structural integrity of F-actin, and possibly in coordinating the activity with *and* among other actin-binding proteins.

CONCLUSION

The rescue of the phenotypic defect in cytokinesis of coronin null cells with expressed GFP- and His-coronins and the dynamic accumulation of coronin into the cleavage furrow indicated that: (1) the modified coronins are physiologically functional, and (2) coronin plays a role in cytokinesis, particularly in the late stage of cytoplasmic cleavage.

ACKNOWLEDGMENTS

We thank Nikon USA, Yokogawa Electronic Corporation, and Hamamatsu Photonics for loan of equipment to S.I. We thank Universal Imaging Corporation for technical support in digital image acquisition. Michael Berger and Alli Raja helped in the preparation of muscle actin. We also thank Bob Valadka and Maya Moody for technical support in printing image panels. E.L.d.H. was supported by a Career Development Award from the American Heart Association and NSF grant 9600923. Y.F. was supported by NIH grant RO1-GM39548.

REFERENCES

- Adachi H, Hasebe T, Yoshinaga K, Ohta T, Sutoh K. 1994. Isolation of *Dictyostelium discoideum* cytokinesis mutants by restriction enzyme-mediated integration of the blasticidin S resistance marker. *Biochem Biophys Res Commun* 205:1808–1814.
- Adachi H, Takahashi Y, Hasebe T, Shirouzu M, Yokoyama S, Sutoh K. 1997. *Dictyostelium* IQGAP-related protein specifically involved in the completion of cytokinesis. *J Cell Biol* 137:891–898.
- Aizawa H, Fukui Y, Yahara I. 1997. Live dynamics of *Dictyostelium* cofilin suggests a role in remodeling actin latticework into bundles. *J Cell Sci* 110:2333–2344.
- Cao L-G, Wang Y-L. 1990. Mechanism of the formation of contractile ring in dividing cultured animal cells. II. Cortical movement of microinjected actin filaments. *J Cell Biol* 111:1905–1911.
- Chalkley HW. 1935. The mechanism of cytoplasmic fission in *Amoeba proteus*. *Protoplasma* 24:607–621.
- Chalkley HW. 1951. Control of fission in *Amoeba proteus* related to the mechanism of cell division. *Ann NY Acad Sci* 51:1303–1310.
- de Hostos EL. 1999. Coronin. In: Kreis T, Vale R, editors. *Guidebook to the cytoskeletal and motor proteins*. Oxford: Oxford University Press, in press.
- de Hostos E L, Bradtke B, Lottespeich F, Guggenheim R, Gerisch G. 1991. Coronin, an actin binding protein of *Dictyostelium discoideum* localized to cell surface projections, has sequence similarities to G protein b subunits. *EMBO J* 10:4097–4104.
- de Hostos E L, Rehfuß C, Bradtke B, Waddell D R, Albrecht R, Murphy J, Gerisch G. 1993. *Dictyostelium* mutants lacking the cytoskeletal protein coronin are defective in cytokinesis and cell motility. *J Cell Biol* 120:163–173.
- De Lozanne A, Spudich JA. 1987. Disruption of the *Dictyostelium* myosin heavy chain gene by homologous recombination. *Science* 236:1086–1091.
- Egelhoff TT, Lee RJ, Spudich JA. 1993. *Dictyostelium* myosin heavy chain phosphorylation sites regulate myosin filament assembly and localization in vivo. *Cell* 75:363–371.
- Faix J, Steinmetz M, Boves H, Kammerer RA, Lottespeich F, Mintert U, Murphy J, Stock A, Aebi U, and Gerisch G. 1996. Cortexillins, major determinants of cell shape and size, are actin-bundling proteins with a parallel coiled-coil tail. *Cell* 86:631–642.
- Fishkind DJ, Wang Y-L. 1993. Orientation and three-dimensional organization of actin filaments in dividing cultured cells. *J Cell Biol* 123:837–848.
- Fujiwara K, Pollard TD. 1976. Fluorescent antibody localization of myosin in the cytoplasm, cleavage furrow and mitotic spindle of human cells. *J Cell Biol* 71:847–875.
- Fujiwara K, Porter ME, Pollard TD. 1978. Alpha-actinin localization in the cleavage furrow during cytokinesis. *J Cell Biol* 79:268–275.
- Fukui Y. 1993. Toward a new concept of cell motility: cytoskeletal dynamics in amoeboid movement and cell division. *Int Rev Cytol* 144:85–127.
- Fukui Y, Inoué S. 1991. Cell division in *Dictyostelium* with special emphasis on actomyosin organization in cytokinesis. *Cell Motil Cytoskeleton* 18:41–54.
- Fukui Y, Inoué S. 1997. Amoeboid movement anchored by eupodia, new actin-rich knobby feet in *Dictyostelium*. *Cell Motil Cytoskeleton* 36:339–354.
- Fukui Y, de Lozanne A, Spudich JA. 1990. Structure and function of the cytoskeleton of a *Dictyostelium* myosin-defective mutant. *J Cell Biol* 110:367–378.
- Fukui Y, de Hostos EL, Inoué S. 1997. Dynamics of GFP-coronin in live *Dictyostelium* observed with real-time confocal optics. *Biol Bull* 193:224–225.
- Fukui Y, Lynch TJ, Brzeska H, Korn ED. 1989. Myosin I is located at

- the leading edges of locomoting *Dictyostelium* amoebae. *Nature* 341:328–331.
- Fukui Y, K-Yumura T, Yumura S. 1999. Myosin II-independent F-actin flow contributes to cell locomotion in *Dictyostelium*. *J Cell Sci* (in press).
- Gerald N, Dai J, Ting-Beall HP, De Lozanne A. 1998. A role for *Dictyostelium* RacE in cortical tension and cleavage furrow progression. *J Cell Biol* 141:483–492.
- Gerisch G, Albrecht R, Heizer C, Hodgkinson S, Maniak M. 1995. Chemoattractant-controlled accumulation of coronin at the leading edge of *Dictyostelium* cells monitored using a green fluorescent protein-coronin fusion protein. *Curr Biol* 5:1280–1285.
- Hacker U, Albrecht R, Maniak M. 1997. Fluid-phase uptake by macropinocytosis in *Dictyostelium*. *J Cell Sci* 110:105–112.
- Heim R, Cubitt AB, Tsien RY. 1995. Improved green fluorescence protein. *Nature* 373:663–664.
- Hiramoto Y. 1970. Rheological properties of sea urchin eggs. *Biorheology* 6:201–234.
- Inoué S, Inoué T. 1996. Digital unsharp masking reveals fine detail in images obtained with new spinning-disk confocal microscope. *Biol Bull* 191:269–270.
- Kitanishi-Yumura T, Fukui Y. 1989. Actomyosin organization during cytokinesis: Reversible translocation and differential redistribution in *Dictyostelium*. *Cell Motil Cytoskeleton* 12:78–89.
- Larochelle DA, Vithalani KK, De Lozanne A. 1996. A novel member of the *rho* family of small GTP-binding protein is specifically required for cytokinesis. *J Cell Biol* 133:1321–1329.
- Larochelle DA, Vithalani KK, De Lozanne A. 1997. Role of *Dictyostelium* racE in cytokinesis: Mutational analysis and localization studies by use of green fluorescent protein. *Mol Biol Cell* 8:935–944.
- Liu T, Williams JG, Clarke M. 1992. Inducible expression of calmodulin antisense RNA in *Dictyostelium* cells inhibits the completion of cytokinesis. *Mol Biol Cell* 3:1403–1413.
- Mabuchi I, Tsukita S, Tsukita S, Sawai T. 1988. Cleavage furrow isolated from newt eggs: Contraction, organization of the actin filaments, and protein components of the furrow. *Proc Natl Acad Sci USA* 85:5966–5970.
- Maniak M, Rauchenberger R, Albrecht R, Murphy J, Gerisch G. 1995. Coronin involved in phagocytosis: dynamics of particle-induced relocalization visualized by a green fluorescent protein tag. *Cell* 83:915–924.
- Manstein DJ, Schuster HP, Morandini P, Hunt DM. 1995. Cloning vectors for the production of proteins in *Dictyostelium discoideum*. *Gene* 162:129–134.
- Marsland D, Landau JV. 1954. The mechanisms of cytokinesis: temperature-pressure studies on the cortical gel system in various marine eggs. *J Exp Zool* 125:507–539.
- Mittal B, Sanger JM, Sanger JW. 1987. Visualization of myosin in living cells. *J Cell Biol* 105:1753–1760.
- Mitchison JM, Swann MM. 1955. The mechanical properties of the cell surface. III. The sea-urchin egg from fertilization to cleavage. *J Exp Biol* 32:734–750.
- Neujahr R, Heizer C, Albrecht R, Ecke M, Schwartz, J-M, Weber I, Gerisch G. 1997. Three-dimensional patterns and redistribution of myosin II and actin in mitotic *Dictyostelium* cells. *J Cell Biol* 139:1793–1804.
- Niswonger ML, O'Halloran TJ. 1997. A novel role for clathrin in cytokinesis. *Proc Natl Acad Sci USA* 94:8575–8578.
- Nunnally MH, D'Angelo JM, Craig SW. 1980. Filamin concentration in cleavage furrow and midbody region: Frequency of occurrence compared with that of alpha-actinin and myosin. *J Cell Biol* 87:219–226.
- Prassler J, Socker S, Marriott G, Heidecker M, Kellermann J, Gerisch G. 1997. Interaction of a *Dictyostelium* member of the plastin/fimbrin family with actin filaments and actin-myosin complexes. *Mol Biol Cell* 8:83–95.
- Rappaport R. 1986. Establishment of the mechanism of cytokinesis in animal cells. *Int Rev Cytol* 105:245–281.
- Rauchenberger R, Hacker U, Murphy J, Niewohner J, Maniak M. 1997. Coronin and vacuolin identify consecutive stages of a late, actin-coated endocytic compartment in *Dictyostelium*. *Curr Biol* 7:215–218.
- Richey B, Cayley DS, Mossing MC, Kolka C, Anderson CF, Farrar TC, Record MT Jr. 1987. Variability of the intracellular ionic environment of *Escherichia coli*. Differences between in vitro and in vivo effects of ion concentrations on protein-DNA interactions and gene expression. *J Biol Chem* 262:7157–7164.
- Salmon ED. 1989. Cytokinesis in animal cells. *Curr Opin Cell Biol* 1:541–547.
- Sanger JM, Mittal B, Pochapin MB, Sanger JW. 1987. Stress fiber and cleavage furrow formation in living cells microinjected with fluorescently labeled -actinin. *Cell Motil Cytoskeleton* 7:209–222.
- Sato N, Yonemura S, Obinata T, Tsukita S, Tsukita S. 1991. Radixin, a barbed end-capping actin-modulating protein, is concentrated at the cleavage furrow during cytokinesis. *J Cell Biol* 113:321–330.
- Scheel J, Ziegelbauer K, Kupke T, Humbel BM, Noegel AA, Gerisch G, Schleicher M. 1989. Hisactophilin, a histidine-rich actin-binding protein from *Dictyostelium discoideum*. *J Biol Chem* 264:2832–2839.
- Schroeder TE. 1968. Cytokinesis: filaments in the cleavage furrow. *Exp Cell Res* 53:272–318.
- Schroeder TE, Otto JJ. 1988. Immunofluorescent analysis of actin and myosin in isolated contractile rings of sea urchin eggs. *Zool Sci* 5:713–725.
- White JG, Borisy GG. 1983. On the mechanisms of cytokinesis in animal cells. *J Theo Biol* 101:289–316.
- Wolpert L. 1960. The mechanics and mechanism of cleavage. *Int Rev Cytol* 10:163–216.
- Yumura S, Fukui Y. 1998. Spatiotemporal dynamics of actin in *Dictyostelium* during cytokinesis and cell locomotion. *J Cell Sci* 111:2097–2108.
- Yumura S, Mori H, Fukui Y. 1984. Localization of actin and myosin for the study of amoeboid movement in *Dictyostelium discoideum* using improved immunofluorescence. *J Cell Biol* 99:894–899.
- Zang J-H, Cavet G, Sabry JH, Wagner P, Moores SL, Spudich JA. 1997. On the role of myosin-II in cytokinesis: Division of *Dictyostelium* cells under adhesive and nonadhesive conditions. *Mol Biol Cell* 8:2617–2629.